

## Accelerated Publications

### Multiple Binding Sites for Tetrahedral Oxyanion Inhibitors of Bovine Spleen Purple Acid Phosphatase<sup>†</sup>

John B. Vincent,<sup>‡</sup> Michael W. Crowder, and Bruce A. Averill\*

Department of Chemistry, University of Virginia, Charlottesville, Virginia 22901

Received December 20, 1991; Revised Manuscript Received January 28, 1992

**ABSTRACT:** The theory of multiple inhibition kinetics has been extended to enzymes for which one inhibitor is noncompetitive and the other exhibits mixed inhibition. Plots of reciprocal velocity versus the concentration of either inhibitor at various fixed concentrations of the second inhibitor are predicted to give parallel lines if binding of the inhibitors is mutually exclusive and intersecting lines if the inhibitors interact at different sites on the enzyme. Application of this analysis to the purple acid phosphatase from bovine spleen in the presence of molybdate (a noncompetitive inhibitor) and phosphate (which exhibits mixed inhibition) results in parallel lines in the reciprocal velocity plots, indicating that phosphate and molybdate compete for a common site; since molybdate is a noncompetitive inhibitor, this site is inferred to be distinct from the site at which substrate binds and is hydrolyzed. Extension of these ideas suggests that phosphate ester substrates should be capable of binding to the molybdate-binding site as well as to the active site, and evidence for substrate inhibition at high substrate concentrations has been obtained. The implications of these findings for interpretation of previous spectroscopic studies of purple acid phosphatase complexes with tetrahedral oxyanions are discussed.

**P**urple (or tartrate-resistant) acid phosphatases (PAP's)<sup>1</sup> constitute a unique class of enzymes that catalyze the hydrolysis of certain phosphate esters, including nucleotide di- and triphosphates, aryl phosphates, and phosphoserine, phosphothreonine, and phosphotyrosine proteins (Vincent & Averill, 1990; Doi et al., 1988b; Antanaitis & Aisen, 1983). The purple phosphatases isolated from mammalian sources are the most thoroughly investigated members of the class, possess highly conserved primary sequences, and contain a dinuclear iron active site. The hydrolysis reaction proceeds via a two-step mechanism involving an acid-labile, base-stable phosphoryl enzyme intermediate (Vincent et al., 1991b). Like other acid phosphatases (Van Etten et al., 1974), the purple acid phosphatases are inhibited by tetrahedral oxyanions. Analysis of the data for inhibition of bovine spleen PAP-catalyzed hydrolysis of *p*-nitrophenyl phosphate by these ox-

yanions and by other phosphate esters revealed that smaller oxyanions (e.g., phosphate and arsenate) inhibit the reaction in a mixed (competitive and noncompetitive) fashion (Scheme I), while larger oxyanions (e.g., tungstate and molybdate) exhibit noncompetitive inhibition (Vincent et al., 1991a). Similarly, optical and EPR spectral studies of oxyanion binding to bovine spleen PAP<sup>2</sup> (Vincent et al., 1991a) and uterine fluid PAP (uteroferin) (David & Que, 1990) have shown the existence of distinct effects upon binding of phosphate and arsenate vs tungstate and molybdate. These differences were also observed in electrochemical studies of oxyanion binding to uteroferin, where the two classes of oxyanions were shown to induce shifts of opposite sign in the reduction potential of the dinuclear cluster (Wang et al., 1991).

Consequently, the existence of two oxyanion binding sites has been postulated (Vincent et al., 1991a). Oxyanion binding to the site at which substrate binds and is hydrolyzed (the

<sup>†</sup> This research was supported by National Institutes of Health Grant GM 32117 (to B.A.A.) and by National Institutes of Health Postdoctoral Fellowship GM 13500 (to J.B.V.).

\* To whom correspondence should be addressed.

<sup>‡</sup> Current address: Department of Chemistry, University of Alabama, Tuscaloosa, AL 35487.

<sup>1</sup> Abbreviations: PAP, purple acid phosphatase; *p*-NPP, *p*-nitrophenyl phosphate; MES, 2-(*N*-morpholino)ethanesulfonic acid; ENDOR, electron nuclear double resonance; EPR, electron paramagnetic resonance.

<sup>2</sup> M. W. Crowder, J. B. Vincent, and B. A. Averill, manuscript in preparation.

"active site") results in competitive inhibition, a blue shift in  $\lambda_{\max}$  of the oxidized enzyme, a red shift of the  $\lambda_{\max}$  of the reduced enzyme at low pH, a broadened, highly temperature-sensitive EPR spectrum, and a negative shift in redox potential, and induces oxidation of the mixed-valence binuclear center. Conversely, oxyanion binding to the other site results in noncompetitive inhibition, small blue shifts in  $\lambda_{\max}$  of the oxidized enzyme, a blue shift in  $\lambda_{\max}$  of the reduced enzyme, a sharp axial EPR spectrum, and a positive shift in redox potential, and stabilizes the mixed-valence binuclear center to aerobic oxidation. Larger oxyanions such as molybdate and tungstate were suggested to occupy only the second site, while smaller oxyanions such as phosphate and arsenate were postulated to be capable of binding to both sites. Given the importance of elucidating the mode of binding of potential substrate analogues such as the tetrahedral oxyanions and the discrepancies in the previously reported modes of inhibition of these anions toward *p*-nitrophenyl phosphate hydrolysis (Vincent et al., 1991a), the use of multiple inhibition kinetics and Yonetani–Theorell plots (Yonetani & Theorell, 1964) has been extended to include systems such as bovine spleen PAP and oxyanions that exhibit noncompetitive and mixed inhibition; the mathematics of systems exhibiting noncompetitive vs competitive inhibition has been treated previously (Segal, 1975). Additionally, inhibition of hydrolysis by the substrate *p*-nitrophenyl phosphate (*p*-NPP) has been investigated.

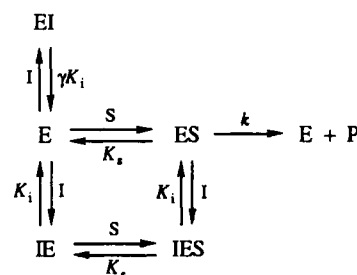
#### MATERIALS AND METHODS

Bovine spleen purple acid phosphatase was isolated as previously described (Vincent et al., 1991a). The concentration of purified enzyme was determined using an extinction coefficient of  $4.08 \times 10^3 \text{ M}^{-1}\text{cm}^{-1}$  for the visible absorption maximum at 536 nm (Vincent et al., 1991a; Campbell et al., 1978). Spectral data for protein determination and kinetics were obtained on a Beckman DU spectrophotometer equipped with a Gilford Model 252-D accessory or on a Hewlett-Packard 845A diode array spectrophotometer. Phosphatase activity was determined as previously described with 0.1 M MES buffer at pH 6.0 (Vincent et al., 1991a; Campbell et al., 1978). Stock solutions of phosphate were made in 0.1 M MES buffer at pH 6.0; stock solutions of molybdate in 0.1 M MES buffer were adjusted to pH 8.0 to avoid formation of polyoxoanion species. For substrate inhibition studies, 0.16 M MES buffer at pH 6.0 without any reductant was utilized. Because of the large range of substrate concentrations, KCl was added to the various buffer and substrate solutions to maintain a constant ionic strength (0.26 M). All kinetics experiments were performed in triplicate.

#### RESULTS AND DISCUSSION

Previously, the mode of inhibition of bovine spleen PAP by the tetraoxyanions<sup>3</sup>  $\text{PO}_4$  and  $\text{AsO}_4$  and the phosphate esters AMP and phosphotyrosine was shown to be mixed competitive–noncompetitive (Scheme I) (Vincent et al., 1991a). This was performed with the aid of Lineweaver–Burk double reciprocal plots and slope and intercept replots, which showed a significant deviation from competitive behavior; in contrast, previous studies on the mode of inhibition of PAP's by  $\text{PO}_4$  had been interpreted as indicating that phosphate acted as a purely competitive inhibitor [reviewed in Vincent et al., (1991a)]. Multiple inhibition studies using  $\text{PO}_4$  and a noncompetitive inhibitor for the bovine enzyme such as  $\text{MoO}_4$  should in principle be able to resolve these discrepancies, by

Scheme I



revealing whether binding of the two inhibitors is mutually exclusive. To date, however, such studies have been limited to cases where both inhibitors are primarily competitive in nature.

If  $I_1$  is an inhibitor that exhibits mixed competitive–noncompetitive inhibition (cf. Scheme I) and  $I_2$  is a simple noncompetitive inhibitor (Scheme I without the upper  $\gamma K_i$  equilibrium), the general rate equation given by Webb (1963) for two inhibitors becomes

$$v_i = V_m / \left( \frac{K_s}{[S]} \left[ 1 + \frac{[I_1]}{\left( \frac{\gamma}{1+\gamma} \right) K_{i_1}} + \frac{[I_2]}{K_{i_2}} + \frac{[I_1][I_2]}{\alpha \left( \frac{\gamma}{1+\gamma} \right) K_{i_1} K_{i_2}} \right] + 1 + \frac{[I_1]}{K_{i_1}} + \frac{[I_2]}{K_{i_2}} + \frac{[I_1][I_2]}{\alpha K_{i_1} K_{i_2}} \right) \quad (1)$$

The mixed inhibitor adds the term  $\gamma/(1+\gamma)$  (Segal, 1975; Vincent et al., 1991a), where  $\gamma$  is the ratio of the binding constants for the competitive and noncompetitive modes of  $I_1$ , and  $\alpha$  is a constant that describes the interaction between  $I_1$  and  $I_2$ . If  $I_1$  and  $I_2$  each prohibit the binding of the other such that both cannot bind simultaneously to the same site, then  $\alpha = \infty$ . However, if the inhibitors can bind simultaneously to the enzyme,  $0 < \alpha < \infty$ ; if the binding of either inhibitor is completely independent of the binding of the second, then  $\alpha = 1$  (Yonetani & Theorell, 1964). Rearranging eq 1 to solve for the reciprocal initial velocity, collecting terms containing  $[I_1]$ , and plotting  $1/v_i$  against  $[I_1]$  at fixed  $[I_2]$  [a Yonetani–Theorell plot (Yonetani & Theorell, 1964)] gives a straight line with a slope of

$$\text{slope} = \frac{K_s}{K_{i_1} V_{\max} [S]} \left( \frac{1}{\frac{\gamma}{1+\gamma}} + \frac{[I_2]}{\alpha \left( \frac{\gamma}{1+\gamma} \right) K_{i_2}} \right) + \frac{1}{V_{\max} K_{i_1}} \left( 1 + \frac{[I_2]}{K_{i_2} \alpha} \right) \quad (2)$$

and an intercept on the  $1/v_i$  axis at

$$\frac{1}{v_i} = \left[ 1 + \frac{[I_2]}{K_{i_2}} \right] \left[ \frac{K_s}{[S]} + 1 \right] \frac{1}{V_{\max}} \quad (3)$$

Consequently, the plot is linear, regardless of the value of  $\alpha$  (the interaction constant between  $I_1$  and  $I_2$ ).

The ratio of the slopes when  $[I_2] \neq 0$  to the slope when  $[I_2] = 0$  is given by

$$\frac{\text{slope}_{[I_2] \neq 0}}{\text{slope}_{[I_2] = 0}} = 1 + \frac{[I_2]}{\alpha K_{i_2}} \quad (4)$$

Thus, if  $\alpha = \infty$ , corresponding to mutually exclusive binding

<sup>3</sup> Use of the abbreviations  $\text{PO}_4$ ,  $\text{MoO}_4$ , etc. is not intended to imply any information as to the degree of protonation of the anion.

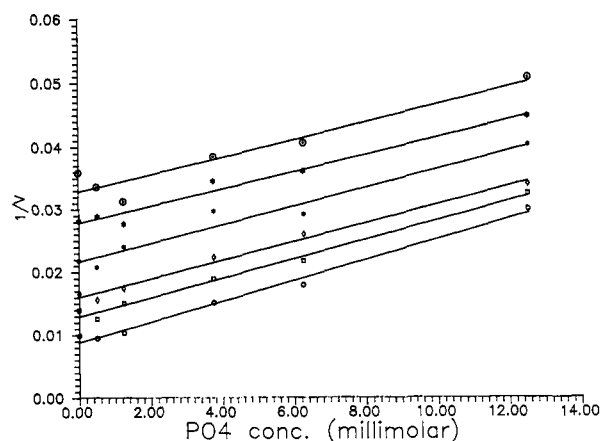


FIGURE 1: Yonetani-Theorell plot of multiple inhibition for *p*-nitrophenyl phosphate hydrolysis by  $\text{MoO}_4$  and  $\text{PO}_4$  as a function of  $[\text{PO}_4]$ . [Substrate] = 10 mM. Molybdate concentrations are (from bottom to top) 0, 0.67, 1.68, 3.25, 5.03, and 6.70  $\mu\text{M}$ .

of  $I_1$  and  $I_2$ , the slopes of lines corresponding to a set of different  $[I_2]$ 's will be identical, giving rise to a series of parallel lines. If the inhibitors bind at different sites such that  $0 < \alpha < \infty$ , then the lines corresponding to different  $[I_2]$ 's will intersect at a point where  $[I_1] = -\alpha [\gamma/(\gamma + 1)]K_{i1}$ .

Taking the reciprocal of eq 1, collecting terms containing  $[I_2]$ , and plotting  $1/v_i$  against  $[I_2]$  at constant  $[I_1]$  also gives a straight line with a slope of

$$\frac{K_s}{V_{\max}K_{i2}[S]} \left( 1 + \frac{[I_1]}{\alpha \left( \frac{\gamma}{1+\gamma} \right) K_{i1}} \right) + \frac{1}{V_{\max}K_{i2}} \left( 1 + \frac{[I_1]}{K_{i1}\alpha} \right) \quad (5)$$

and an intercept on the axis at  $1/v_i$

$$\frac{1}{v_i} = \frac{K_s}{V_{\max}[S]} \left( 1 + \frac{[I_1]}{\left( \frac{\gamma}{1+\gamma} \right) K_{i1}} \right) + \frac{1}{V_{\max}} \left( 1 + \frac{[I_1]}{K_{i1}} \right) \quad (6)$$

The ratio of the slopes is given by

$$\frac{\text{slope}_{[I_1] \neq 0}}{\text{slope}_{[I_1] = 0}} = 1 + \left( \frac{[I_1]}{\alpha K_{i1}} \right) \left[ \frac{\frac{K_s}{[S]} \left( \frac{\gamma}{1+\gamma} \right) + 1}{\frac{K_s}{[S]} + 1} \right] \quad (7)$$

Consequently, if  $\alpha = \infty$ , as it must be if both  $I_1$  and  $I_2$  bind to a common site, the result is again a series of parallel lines. If  $0 < \alpha < \infty$ , the lines corresponding to  $[I_1] = 0$  and  $[I_1] \neq 0$  will intersect at a point where  $[I_1] = -\alpha K_{i1}$ . Therefore, independent of whether the Yonetani and Theorell plots are present in terms of  $[I_1]$  or  $[I_2]$ , the results will be parallel lines if  $I_1$  and  $I_2$  exhibit mutually exclusive binding. Intersecting lines in the plots require that both inhibitors bind to different sites, although the binding of one inhibitor may affect the binding of the other.<sup>4</sup>

In the case of  $I_1$  exhibiting mixed noncompetitive-competitive inhibition (e.g.,  $\text{PO}_4$ ) and  $I_2$  being a noncompetitive

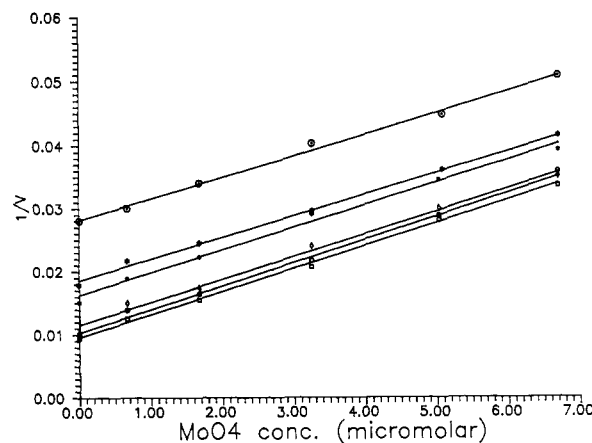


FIGURE 2: Yonetani-Theorell plot of multiple inhibition of *p*-nitrophenyl phosphate hydrolysis by  $\text{MoO}_4$  and  $\text{PO}_4$  as a function of  $[\text{MoO}_4]$ . [Substrate] = 10 mM. Phosphate concentrations are (from bottom to top) 0, 0.50, 1.25, 3.75, 6.25, and 12.5 mM.

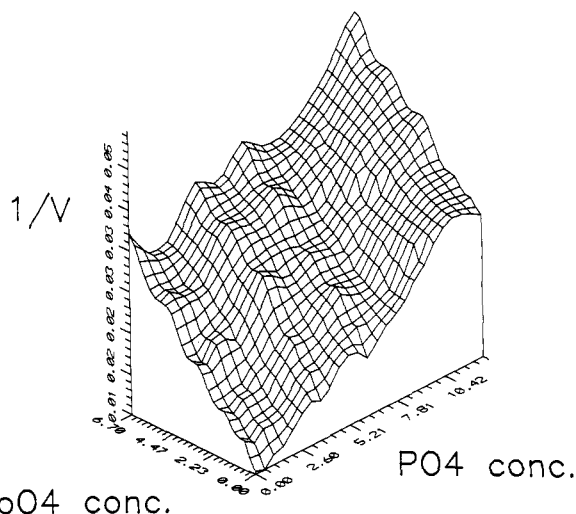


FIGURE 3: Plot of reciprocal velocity as a function of  $[\text{MoO}_4]$  and  $[\text{PO}_4]$ . [Substrate] = 10 mM.

inhibitor (e.g.,  $\text{MoO}_4$ ), both anions compete directly for the molybdate-binding site (but not for the active site), resulting in an expected value of  $\infty$  for  $\alpha$  and parallel lines in the Yonetani and Theorell plots. The results for inhibition of hydrolysis of *p*-NPP by bovine spleen PAP with phosphate and molybdate are presented in Figures 1 and 2. Within experimental error, all lines in the Yonetani and Theorell plots, independent of whether the data are plotted as a function of  $[I_1]$  or  $[I_2]$ , are *parallel*. Hence,  $\alpha = \infty$ , and the tetrahedral oxyanions compete directly for a common site (the molybdate-binding site) in accordance with Scheme I. (It should be noted explicitly that while Scheme I shows the inhibitor binding to the E-S complex, steady-state kinetics studies cannot distinguish between this and binding of the inhibitor to a species derived from the E-S complex during the catalytic reaction.)

If  $\alpha = \infty$ , the general rate equation (eq 1) can be simplified and rearranged to give

$$0 = [I_1] \left[ \frac{1}{V_{\max}K_{i1}} \right] \left[ \frac{K_s}{[S] \left( \frac{\gamma}{1+\gamma} \right)} + 1 \right] + [I_2] \left[ \frac{1}{V_{\max}K_{i2}} \right] \left[ \frac{K_s}{[S]} + 1 \right] + \frac{-1}{V_i} + \frac{1}{V_{\max}} \left[ \frac{K_s}{[S]} + 1 \right] \quad (8)$$

<sup>4</sup> These conclusions do not depend on whether  $I_2$  exhibits noncompetitive or uncompetitive inhibition. Although the algebraic form of the relevant equations differs in the latter case, the results of eqs 4 and 7 for the case where  $\alpha = \infty$  are the same in both cases, producing parallel lines in the reciprocal velocity vs  $[I]$  plots.

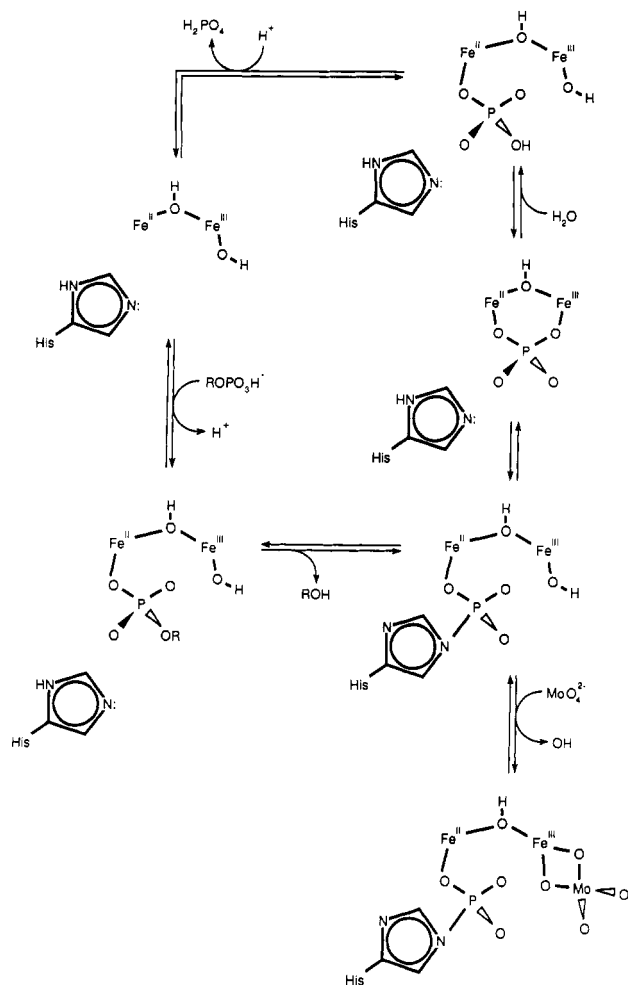
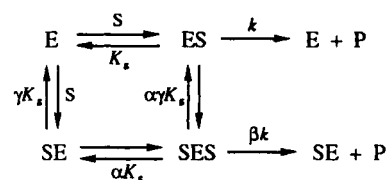


FIGURE 4: Proposed mechanism for phosphate ester hydrolysis by the purple acid phosphatase from bovine spleen, indicating possible modes of binding for the tetraoxanion inhibitors phosphate and molybdate.

which has the form of a plane; i.e.,  $0 = Ax + By + Cz + D$ . A plot of  $1/v_i$  as a function of  $[\text{PO}_4]$  ( $I_1$ ) and of  $[\text{MoO}_4]$  ( $I_2$ ) for the inhibition of spleen PAP is shown in Figure 3 and clearly takes the overall form of a plane (the ripples reflect experimental uncertainties), again confirming the fact that  $\text{MoO}_4$  and  $\text{PO}_4$  exhibit mutually exclusive binding.

Given that  $\text{MoO}_4$  exhibits purely noncompetitive inhibition, the common binding site for  $\text{MoO}_4$  and  $\text{PO}_4$  (i.e., that occupied by I in the lower portion of Scheme I) must be distinct from the site at which substrate binds and is hydrolyzed (the active site). In other words, binding of oxyanions to the second site does *not* prevent binding of substrate, although it does impede the hydrolysis reaction. Since  $\text{MoO}_4$  exhibits noncompetitive inhibition, this implies that  $\text{MoO}_4$  binding both decreases the rate of hydrolysis of bound substrate (affecting  $V_{\max}$ ) and decreases the affinity of the enzyme for substrate (affecting  $V_{\max}/K_m$ ) (Cleland, 1970). A plausible hypothesis for the noncompetitive binding mode of oxyanion inhibitors is shown in Figure 4; this incorporates the recent finding that the enzyme contains an ionizable group capable of forming a base-stable, covalent phosphoryl enzyme intermediate (Vincent et al., 1991b). In this drawing, a significant parallel between the chemistry of the Zn-containing alkaline phosphatases (Kim & Wyckoff, 1991) and the PAP's is proposed, with the ferric ion used to generate a hydroxide nucleophile at pH 5 for attack on the phosphoryl enzyme intermediate (Vincent et al., 1992), rather than directly on the phosphate ester substrate as proposed by Dietrich et al. (1991). Binding of  $\text{MoO}_4$  to the ferric

Scheme II



center as shown would inhibit hydrolysis of the phosphoryl enzyme intermediate without preventing substrate binding, although electrostatic effects might be expected to decrease the affinity of the enzyme-molybdate complex for the anionic substrate.

The kinetics results provide a basis for interpretation of previous spectroscopic studies of the interaction of tetrahedral oxyanions with the binuclear iron center of PAP's. ENDOR studies on the PAP from porcine uterine fluid in the presence of  $\text{MoO}_4$  indicate that  $\text{MoO}_4$  binds to the dinuclear iron center (Doi et al., 1988a), while recent direct EPR studies have shown that  $\text{PO}_4$  binds directly to the ferric iron in the  $\text{FeZn}$  form of the porcine enzyme (and by implication to the diiron center of the native enzyme) (David & Que, 1990). According to Scheme I and Figure 4, the  $\text{MoO}_4$  results reflect binding of the oxyanion to a site that is distinct from the substrate binding site. In contrast, the  $\text{PO}_4$  results are probably best interpreted in terms of a bridging phosphate as shown in Figure 4. This is also consistent with available Mössbauer data, which indicate that  $\text{PO}_4$  binding perturbs both iron atoms (Pyrz et al., 1986).

Finally, we have shown previously that phosphotyrosine is an excellent substrate for bovine spleen PAP and exhibits mixed inhibition of *p*-NPP hydrolysis (Vincent et al., 1991a), suggesting that it also binds to two distinct sites as shown in Scheme I. The structural similarity between phosphotyrosine and *p*-NPP suggests that the latter should also be capable of binding to both sites, implying that bovine spleen PAP should exhibit substrate inhibition at high  $[\text{p-NPP}]$ . Adapting the general scheme for substrate inhibition (Scheme II) (Webb, 1963), such that *p*-NPP is a noncompetitive inhibitor of its own hydrolysis in agreement with Scheme I, and solving the corresponding kinetics equation (Webb, 1963) gives

$$\frac{1}{v_i} = \left[ \frac{K_s}{V_{\max} [S]} + \frac{1}{V_{\max}} \right] + \frac{1}{\gamma V_{\max}} \left[ 1 + \frac{[S]}{K_s} \right] \quad (9)$$

In deriving this equation, values of  $\alpha = 1$  and  $\beta = 0$  in Scheme II have been used, as derived from Lineweaver-Burk plots of the inhibition data (Vincent et al., 1991a). Plots of  $1/v_i$  versus  $1/[S]$  should therefore be linear at low substrate concentrations, with the linear function having slope  $\sim K_s/V_{\max}$  and intercepting the  $1/v_i$  axis at  $1/v_i = 1/V_{\max}$  upon extrapolation. However, at high  $[S]$  the plot should display curvature as a result of the rapid increase in  $1/v_i$ . A double reciprocal plot of the hydrolysis of *p*-NPP by bovine spleen PAP is shown in Figure 5; substrate inhibition is clearly evident at high  $[S]$ .

The solid line in Figure 5 is a curve calculated for  $\gamma = 1000$ ,  $\alpha = 1$ , and  $\beta = 0$  and suggests that a value of ca. 1000 is a reasonable estimate for the value of  $\gamma$ . The data in Figure 5 were obtained under conditions designed to minimize artifacts caused by changes in variables such as ionic strength, which can in some cases mimic the effect of substrate inhibition. Although not conclusive in themselves, the substrate inhibition results are in agreement with the existence of two distinct binding sites for both  $\text{PO}_4$  and phosphate ester substrates. In support of this, substrate inhibition by  $\alpha$ -naphthyl phosphate has also been reported recently (Dietrich et al., 1991). Using the limited number of data reported, the value

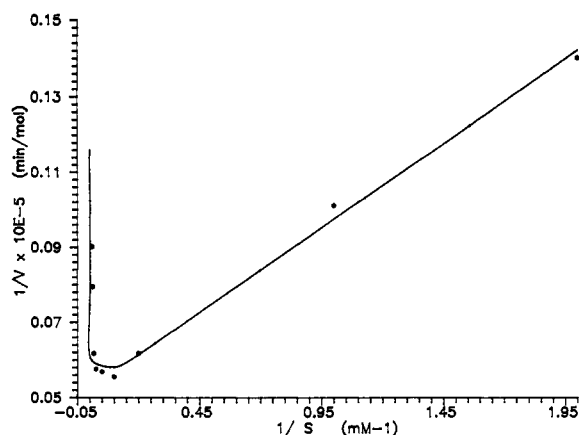


FIGURE 5: Double reciprocal plot for *p*-nitrophenyl phosphate hydrolysis.

of  $\gamma$  for this system appears to be 35–45.

Scheme I and Figure 4 both suggest the possible existence of ternary complexes derived from substrate and inhibitors such as  $\text{MoO}_4$ . Spectroscopic experiments are currently in progress in an attempt to detect the existence of such ternary species in order to confirm independently the results of the kinetics investigations.

#### ACKNOWLEDGMENTS

We acknowledge D. Crans for bringing the Yonetani and Theorell paper to our attention and thank J. N. Demas for assistance with the plot in Figure 3.

Registry No. *p*-NPP, 330-13-2; AP, 9001-77-8;  $\text{MoO}_4^{2-}$ , 14259-85-9;  $\text{PO}_4^{3-}$ , 14265-44-2.

#### REFERENCES

Antanaitis, B. C., & Aisen, P. (1983) *Adv. Inorg. Biochem.* 5, 111–136.

- Campbell, H. D., Dionysios, D. A., Keough, D. T., Wilson, B. F., de Jersey, J., & Zerner, B. (1978) *Biochem. Biophys. Res. Commun.* 82, 615–620.
- Cleland, W. W. (1970) *Enzymes (3rd Ed.)* 2, 1–50.
- David, S. S., & Que, L., Jr. (1990) *J. Am. Chem. Soc.* 112, 6455–6463.
- Dietrich, M., Münsterman, D., Suerbaum, H., & Witzel, H. (1991) *Eur. J. Biochem.* 199, 105–113.
- Doi, K., McCracken, J., Peisach, J., & Aisen, P. (1988a) *J. Biol. Chem.* 263, 5757–5763.
- Doi, K., Antanaitis, B. C., & Aisen, P. (1988b) *Struct. Bonding* 70, 1–26.
- Kim, E. E., & Wyckoff, H. W. (1991) *J. Mol. Biol.* 218, 449–464.
- Pyrz, J. W., Sage, T. J., Debrunner, P. G., & Que, L., Jr. (1986) *J. Biol. Chem.* 261, 11015–11020.
- Segal, I. H. (1975) *Enzyme Kinetics: Behavior and Analysis of Rapid Equilibrium and Steady-State Enzyme Systems*, p 493, Wiley, New York.
- Van Etten, R. L., Waymack, P. P., & Rehkop, D. M. (1974) *J. Am. Chem. Soc.* 96, 6782–6785.
- Vincent, J. B., & Averill, B. A. (1990) *FASEB J.* 4, 3009–3014.
- Vincent, J. B., Crowder, M. W., & Averill, B. A. (1991a) *Biochemistry* 30, 3025–3034.
- Vincent, J. B., Crowder, M. W., & Averill, B. A. (1991b) *J. Biol. Chem.* 266, 17737–17740.
- Vincent, J. B., Crowder, M. W., & Averill, B. A. (1992) *Trends Biochem. Sci.* (in press).
- Wang, D. L., Holz, R. C., David, S. S., Que, L., Jr., & Stankovich, M. R. (1991) *Biochemistry* 30, 8187–8194.
- Webb, J. L. (1963) *Enzyme and Metabolic Inhibitors*, Vol. 1, Academic Press, New York.
- Yonetani, T., & Theorell, H. (1964) *Arch. Biochem. Biophys.* 106, 243–251.